NLRP3 signaling drives macrophage-induced adaptive immune suppression in pancreatic carcinoma

Donnele Daley,[1]* Vishnu R. Mani,[1]* Navyatha Mohan,[1] Neha Akkad,[1] Gautam S.D. Balasubramania Pandian,[1] Shivraj Savadkar,[1] Ki Buom Lee,[1] Alejandro Torres-Hernandez,[1] Berk Aykut,[1] Brian Diskin,[1] Wei Wang,[1] Mohammad S. Farooq,[1] Arif I. Mahmud,[1] Gregor Werba,[1] Eduardo J. Morales,[1] Sarah Lall,[1] Benjamin J. Wadowski,[1] Amanda G. Rubin,[1] Matthew E. Berman,[1] Rajkishen Narayanan,[1] Mautin Hundeyin,[1] and George Miller[1,2]

[1]S.A. Localio Laboratory, Department of Surgery and [2]Department of Cell Biology, New York University School of Medicine, New York, NY 10016

The tumor microenvironment (TME) in pancreatic ductal adenocarcinoma (PDA) is characterized by immune tolerance, which enables disease to progress unabated by adaptive immunity. However, the drivers of this tolerogenic program are incompletely defined. In this study, we found that NLRP3 promotes expansion of immune-suppressive macrophages in PDA. NLRP3 signaling in macrophages drives the differentiation of $CD4^+$ T cells into tumor-promoting T helper type 2 cell (Th2 cell), Th17 cell, and regulatory T cell populations while suppressing Th1 cell polarization and cytotoxic $CD8^+$ T cell activation. The suppressive effects of NLRP3 signaling were IL-10 dependent. Pharmacological inhibition or deletion of NLRP3, ASC (apoptosis-associated speck-like protein containing a CARD complex), or caspase-1 protected against PDA and was associated with immunogenic reprogramming of innate and adaptive immunity within the TME. Similarly, transfer of PDA-entrained macrophages or T cells from $NLRP3^{-/-}$ hosts was protective. These data suggest that targeting NLRP3 holds the promise for the immunotherapy of PDA.

INTRODUCTION

Pancreatic ductal adenocarcinoma (PDA) is a devastating disease in which the mortality rate approaches the incidence rate (Yadav and Lowenfels, 2013). PDA is almost invariably associated with a modest T cell infiltrate, which can have divergent effects on disease progression by either combating cancer growth via antigen-restricted tumoricidal immune responses or, more commonly, by promoting tumor progression via induction of immune suppression (Clark et al., 2007; Zheng et al., 2013). Specifically, T cell differentiation within the PDA tumor microenvironment (TME) is an important determinant of disease outcome. T helper type 1 cell (Th1 cell)–polarized $CD4^+$ T cells mediate tumor protection in mouse models of PDA and are associated with prolonged survival in human disease (De Monte et al., 2011). Conversely, Th2 cell–polarized $CD4^+$ T cells promote PDA progression in mice, and intratumoral $CD4^+$ Th2 cell infiltrates correlate with reduced survival in human PDA (Fukunaga et al., 2004; De Monte et al., 2011; Ochi et al., 2012b). Similarly, $CD4^+CD25^+$ $Foxp3^+$ regulatory T cells (T reg cells) enable tumor immune escape, and Th17 cell–differentiated $CD4^+$ T cells facilitate epithelial cell proliferation in PDA (Hiraoka et al., 2006; McAllister et al., 2014). However, regulation of the balance between immunogenic and tolerogenic T cell polarization in the PDA TME is uncertain.

The NOD-like receptor family pyrin domain–containing 3 (NLRP3) inflammasome is a multimeric complex involved in the induction of innate inflammatory responses. The complex consists of the NLRP3 protein, which acts as a sensor for the activation of the inflammasome, and an apoptosis-associated speck-like protein containing a CARD complex (ASC), which recruits pro–caspase-1 through its CARD domain. Pro–caspase-1 is then converted to caspase-1, which, in turn, cleaves both pro–IL-1β and pro–IL-18 to their active forms. IL-1β and IL-18 serve to promote inflammation by recruiting additional inflammatory cells. Thus, NLRP3 signaling sustains sterile inflammation in the homeostatic state and under diverse pathological conditions. Conversely, NLRP3 deficiency mitigates susceptibility to myocardial infarction, acute renal injury, graft-versus-host disease, sterile liver inflammation, and a host of autoimmune diseases (Fowler et al., 2014; Komada et al., 2015; Lugrin et al., 2015; Kobayashi et al., 2016). In the pancreas, NLRP3 activation was found to be necessary for the development of experimental acute pancreatitis and to significantly contribute to obesity-induced insulin resistance (Hoque et al., 2011;

*D. Daley and V.R. Mani contributed equally to this paper.

Correspondence to George Miller: george.miller@nyumc.org

Abbreviations used: H&E, hematoxylin and eosin; PDA, pancreatic ductal adenocarcinoma; PSC, pancreatic stellate cell; TAM, tumor-associated macrophage; TME, tumor microenvironment; NLRP3, NOD-like receptor family pyrin domain–containing 3.

The Rockefeller University Press $30.00
J. Exp. Med. 2017 Vol. 214 No. 6 1711–1724
https://doi.org/10.1084/jem.20161707

Vandanmagsar et al., 2011). However, the role of NLRP3 signaling in the development or progression of PDA is uncertain.

Our preliminary investigations showed that NLRP3 is markedly up-regulated in macrophages in PDA. We postulated that NLRP3 signaling underlies the propensity of tumor-associated macrophages (TAMs) to support immune-suppressive $CD4^+$ T cell polarization in the TME. We also speculated that blockade of NLRP3 signaling would reprogram the inflammatory TME toward a tumor-protective phenotype. We found that NLRP3 signaling in macrophages directs tolerogenic T cell differentiation in PDA. Our data suggest that targeting the NLRP3 inflammasome holds the promise for successful immunotherapy of PDA.

RESULTS

High NLRP3 signaling in subsets of PDA-associated macrophages in mice and humans

To assess the relevance of NLRP3 to PDA, we examined NLRP3 signaling in a slowly progressive mouse model of PDA using $p48^{Cre}$;$LSL\text{-}Kras^{G12D}$ (KC) mice, which express oncogenic *Kras* in their pancreatic progenitor cells (Hingorani et al., 2003), in an invasive orthotopic PDA model using tumor cells derived from $Pdx1^{Cre}$;$LSL\text{-}Kras^{G12D}$;$Tp53^{R172H}$ (KPC) mice, which express both mutant *Kras* and *p53* (Hingorani et al., 2005), and in human disease. Western blotting showed up-regulated expression of IL-18 and IL-1β in pancreata of KC mice compared with WT (Fig. 1 A). Immunofluorescence microscopy suggested high NLRP3 expression in myeloid cells in pancreata of KC mice (Fig. 1 B). Flow cytometry analysis confirmed up-regulated NLRP3 expression in pancreas-infiltrating macrophages in KC mice compared with minimal expression in splenic macrophages (Fig. 1 C). Moreover, $CD206^+MHCII^-$ M2-like macrophages, which were increased in prevalence in pancreatic intraepithelial neoplasia lesions compared with spleen (Fig. 1 E), expressed high NLRP3 and IL-1β, whereas NLRP3 and IL-1β expression were low in $CD206^-MHCII^+$ M1-like macrophages in pancreata of KC mice (Fig. 1 E). In orthotopic KPC tumors, NLRP3 and IL-1β were also up-regulated in $CD206^+MHC\ II^-$ M2-like TAMs compared with $CD206^-MHCII^+$ M1-like TAMs (Fig. 1 F). NLRP3 was minimally expressed in macrophages in nontumor-bearing pancreata (Fig. 1 G). In human PDA, immunohistochemical analysis confirmed high NLRP3 expression in the TME (Fig. 1 H). Furthermore, similar to mice, PDA-infiltrating $CD15^+$ monocytic cells expressed markedly higher NLRP3 than their counterparts in PBMCs (Fig. 1 I).

Because macrophages in the PDA TME express higher NLRP3 than their cellular counterparts in the mouse spleen, normal pancreas, or in human PBMCs, we postulated that pancreatic carcinoma cells may directly up-regulate NLRP3 expression in TAMs. To test this, we co-incubated KPC-derived tumor cells with splenic macrophages and assessed the change in macrophage NLRP3 expression. PDA cells increased the M2 polarization of macrophages (Fig. 1 J). Contrary to our hypothesis, tumor cells did not directly up-regulate macrophage expression of NLRP3 (Fig. 1 J). However, we found that TGF-β and, to a lesser extent, TNF, which are each overexpressed in the PDA TME (Zhang et al., 2012; Greco et al., 2015), up-regulate NLRP3 expression in BMDMs (Fig. 1 K). Accordingly, serial blockade of TGF-β in vivo in PDA-bearing mice reduced NLRP3 expression ∼3-fold and concomitantly lowered CD206 expression in TAMs (Fig. 1 L).

NLRP3 deletion is protective against PDA

To determine whether NLRP3 signaling is required for the normal progression of pancreatic oncogenesis, we crossed $NLRP3^{-/-}$ mice with KC animals to generate $KC;NLRP3^{-/-}$ mice. NLRP3 deletion delayed malignant progression. Compared with $KC;NLRP3^{+/+}$ controls, age-matched $KC;NLRP3^{-/-}$ pancreata exhibited a slower rate of development of pancreatic dysplasia (Fig. 2 A), reduced pancreatic weights (Fig. 2 B), diminished peritumoral fibrosis (Fig. 2 C), and extended survival (Fig. 2 D). To investigate whether NLRP3 deletion is protective in a more aggressive model of PDA, WT and $NLRP3^{-/-}$ mice were challenged with an orthotopic injection of KPC-derived tumor cells and sacrificed at 3 wk. Orthotopic KPC tumor growth was significantly reduced in pancreata of $NLRP3^{-/-}$ mice (Fig. 2 E). Collectively, these data suggest that NLRP3 signaling promotes accelerated progression of pancreatic neoplasia and that targeting NLRP3 may hold therapeutic promise.

ASC, caspase-1 deletion, or pharmacologic inhibition of NLRP3 is protective against PDA

Because NLRP3 complexes with ASC and caspase-1 to mediate inflammation, we postulated that targeting either ASC or caspase-1 would also confer protection against PDA. Consistent with our hypothesis, orthotopically implanted PDA tumors grew at reduced rates in both $ASC^{-/-}$ and $Casp\text{-}1^{-/-}$ mice (Fig. 3 A). Furthermore, because genetic deletion of NLRP3 or components of the inflammasome have limited direct translational application to treatment of human disease, we tested whether pharmacologic inhibition of NLRP3 activation would be similarly protective. KC mice were serially treated for 8 wk with Glybenclamide, which blocks the maturation of caspase-1 and pro–IL-1β (Lamkanfi et al., 2009). Glybenclamide was protective against pancreatic oncogenesis (Fig. 3 B). Administration of CRID3, which blocks ASC oligomerization in the NLRP3 inflammasome (Coll et al., 2011), was not significantly protective against PDA as a single agent; however, CRID3 offered synergistic efficacy when combined with TLR9 inhibition (Fig. 3 C). By contrast, selective deletion of the NOD2 inflammasome, which functions independently of NLRP3, was not protective in PDA in the KC or orthotopic KPC models (Fig. 4), suggesting specificity of effects to NLRP3.

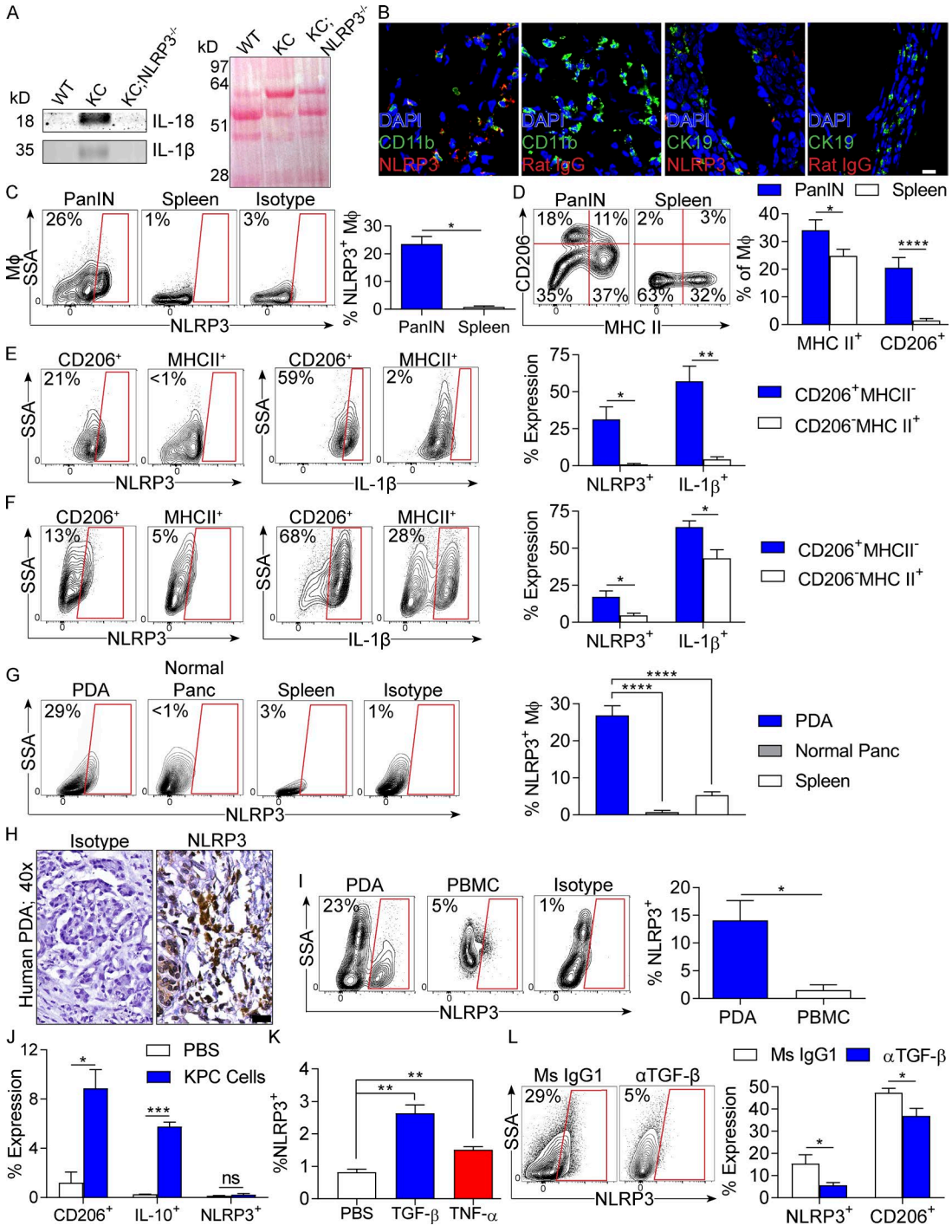

Figure 1. **NLRP3 expression in human and mouse PDA.** (A) Lysate from 3-mo-old WT, KC, and KC;NLRP3$^{-/-}$ mice were tested for expression of IL-1β and IL-18 by Western blotting. Ponceau staining is shown. Experiments were repeated three times. Representative data are shown. (B) Frozen sections of pancreata of mouse PDA tumors were tested for coexpression of CD11b and NLRP3 or CK19 and NLRP3 compared with respective isotype controls. Bar, 10 µm. (C) F4/80^{+}Gr1^{-}CD11c^{-}CD11b^{+} macrophages from pancreata or spleen macrophages from 3-mo-old KC mice were tested for expression of NLRP3 compared with isotype controls. (D) Macrophages from pancreata or spleen of KC mice were tested for coexpression of MHC II and CD206. (E) MHC II^{-}CD206^{+} and MHC II^{+}CD206^{-} pancreatic macrophage subsets from 3-mo-old KC mice were gated and tested for expression of NLRP3 and IL-1β. Representative and quantitative data are shown. Positive gates are based on isotype controls (not depicted). (F) MHC II^{-}CD206^{+} and MHC II^{+}CD206^{-} TAM subsets from WT mice bearing orthotopic PDA were gated and tested for expression of NLRP3 and IL-1β. (G) Macrophages from WT control pancreata or pancreata or spleen of WT mice harboring orthotopic KPC tumors were tested for expression of NLRP3. (H) Paraffin-embedded sections of human PDA were tested for expression of NLRP3 compared with isotype control. Bar, 20 µm. (I) CD15^{+} monocytic cells from single-cell suspensions of human PDA or PBMCs were gated by flow

NLRP3-activated TAMs do not have direct proliferative effects on pancreatic tumor cells or induce PSC activation

We postulated that NLRP3-activated TAMs may directly induce tumor cell proliferation in PDA. To test this, we co-cultured NLRP3$^{+/+}$ and NLRP3$^{-/-}$ macrophages with KPC-derived tumor cells. TAMs induced tumor cell proliferation in vitro as previously reported (Pollard, 2004). However, WT TAMs did not induce higher tumor cell proliferation compared with NLRP3$^{-/-}$ TAMs (Fig. 5 A). Similarly, exogenous NLRP3 ligation using alum did not endow macrophages with the capacity to differentially promote tumor cell proliferation (Fig. 5 A). Pancreatic stellate cells (PSCs) did not express NLRP3 (not depicted). Nevertheless, because we observed that NLRP3 deletion mitigated stromal fibrosis in vivo, we postulated that NLRP3 signaling in TAMs may increase their ability to activate PSCs. However, neither NLRP3 deletion nor NLRP3 ligation influenced the capacity of TAMs to promote PSC proliferation (Fig. 5 B) or expression of proinflammatory cytokines (Fig. 5 C). Collectively, these data suggest that NLRP3-activated TAMs do not directly enhance oncogenic properties in transformed epithelial cells or PSCs.

NLRP3 deletion induces immunogenic reprogramming of tumor-infiltrating macrophages

We postulated that NLRP3 signaling may promote immune suppression within the PDA TME. Assessment of the innate immune infiltrate in orthotopic KPC tumors in WT and NLRP3$^{-/-}$ hosts suggested that NLRP3 deletion reduced the fraction of TAMs but did not alter the fraction of CD11c^{+}MHCII^{+} DCs or Gr1^{+}CD11b^{+} neutrophils and inflammatory monocytes in the TME (Fig. 6 A). Furthermore, NLRP3 deletion up-regulated TNF expression in TAMs but lowered IL-10 and CD206 expression, suggesting that NLRP3 deletion reprograms PDA-infiltrating macrophages toward an M1-like phenotype (Fig. 6, B and C). We postulated that the immunogenic differentiation of TAMs associated with NLRP3 deletion may reverse the immune-suppressive T cell phenotype characteristic of PDA (Seifert et al., 2016a). To test this using in vitro modeling, we activated spleen-derived CD8^{+} T cells using CD3/CD28 coligation and selectively co-cultured them with either NLRP3$^{+/+}$ or NLRP3$^{-/-}$ TAMs harvested from orthotopic KPC tumors. Consistent with our hypothesis, whereas WT TAMs abrogated IFN-γ and CD44 expression in αCD3/CD28-stimulated CD8^{+} T cells, NLRP3$^{-/-}$ TAMs exhibited no inhibitory effects on T cell activation (Fig. 6, D and E). To determine whether NLRP3 signaling in TAMs adversely affects their capacity to induce adaptive immune responses to tumor antigen, WT and NLRP3$^{-/-}$ TAMs were harvested from orthotopic KPC tumors, loaded with OVA$_{257–264}$ peptide, and used to activate OT-I T cells. WT TAMs only weakly induced antigen-restricted CD8^{+} T cell proliferation and were deficient in promoting T cell activation based on low expression of T-bet, CD44, and IFN-γ; conversely, NLRP3$^{-/-}$ TAMs induced vigorous CD8^{+} T cell proliferation and promoted a cytotoxic T cell phenotype (Fig. 6, F–I). Notably, IL-10 blockade rescued the capacity of NLRP3$^{+/+}$ TAMs to present antigen (Fig. 6, F–I).

To definitively determine whether TAMs are responsible for NLRP3-mediated tumorigenesis, we serially neutralized macrophages in orthotopic PDA-bearing WT and NLRP3$^{-/-}$ hosts. Macrophage depletion was protective against PDA in WT hosts, as we have previously reported (Seifert et al., 2016a); however, macrophage neutralization did not offer further tumor protection in the context of NLRP3 deletion (Fig. 6 J). Similarly, adoptive transfer of WT TAMs coincident with KPC tumor challenge in NLRP3$^{-/-}$ hosts resulted in an accelerated tumor growth rate compared with transfer of NLRP3$^{-/-}$ TAMs (Fig. 6 K). Moreover, transfer of NLRP3$^{-/-}$ TAMs resulted in upward skewing of the CD8/CD4 ratio in the TME and enhanced intratumoral CD4^{+} and CD8^{+} T cell activation compared with adoptive transfer of WT TAMs (Fig. S1).

We previously reported that neutrophils and inflammatory monocytes restrain T cell immunogenicity in PDA (Pylayeva-Gupta et al., 2012; Zambirinis et al., 2015). Similar to TAMs, neutrophils and inflammatory monocytes also up-regulated NLRP3 expression in PDA (Fig. S2 A). However, the phenotype of neutrophils and inflammatory monocytes was unchanged (Fig. S2 B), and their T cell inhibitory function was not diminished by NLRP3 deletion (Fig. S2, C and D).

NLRP3 governs T cell differentiation within the PDA TME

To test whether NLRP3 deletion in situ leads to enhanced T cell immunogenicity within the PDA TME, we interrogated CD4^{+} and CD8^{+} T cell phenotype in PDA-bearing WT and NLRP3$^{-/-}$ pancreata. Consistent with our macrophage adoptive transfer experiments, NLRP3 deletion increased the CD8/CD4 ratio in PDA tumors (Fig. 7 A). Furthermore, NLRP3 deletion resulted in CD4^{+} T cell reprogramming toward an immunogenic Th1 cell phe-

cytometry and tested for expression of NLRP3. Representative contour plots and quantitative data from six patients are shown. (J) Splenic macrophages from WT mice were cultured alone or in a 5:1 ratio with KPC-derived tumor cells. At 24 h, macrophages were tested for expression of CD206, IL-10, and NLRP3. (K) Similarly, BMDMs from WT mice were stimulated with recombinant TGF-β or TNF and tested for NLRP3 expression. (L) Orthotopic PDA-bearing mice were serially treated with a neutralizing TGF-β mAb or isotype control. Tumors were harvested on day 21, and expression of NLRP3 and CD206 in TAMs was determined by flow cytometry. n = 5/group. All mouse experiments were repeated a minimum of twice using five mice per experimental group. Littermate controls were used. Unpaired Student's t test was used for statistical analyses. *, P < 0.05; **, P < 0.01; ***, P < 0.001; ****, P < 0.0001. Data are presented as mean ± standard error. MΦ, macrophage; Ms, mouse; Panc, pancreas; PanIN, pancreatic intraepithelial neoplasia; SSA, side scatter.

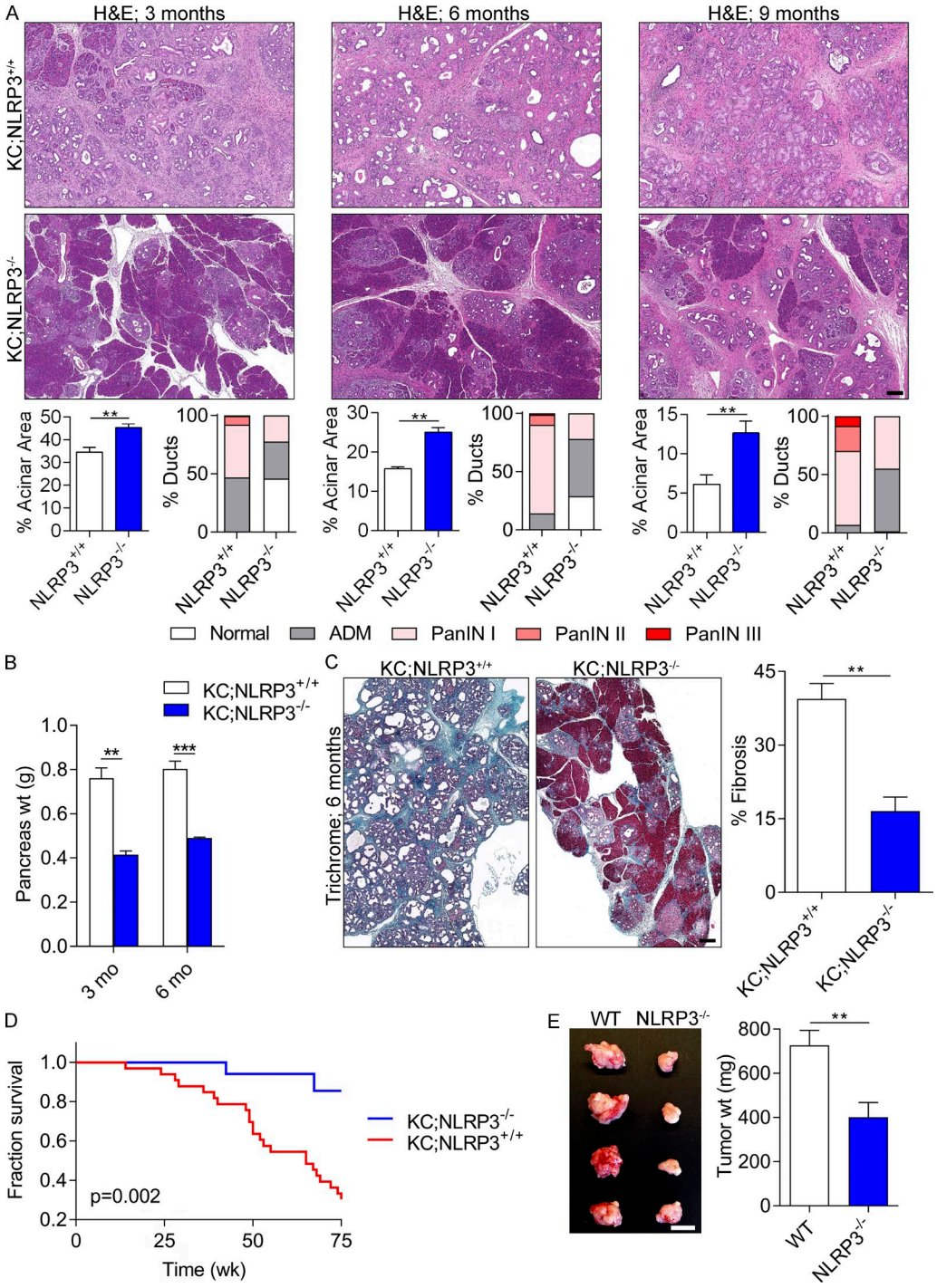

Figure 2. **NLRP3 deletion or blockade is protective against PDA.** (A) KC;NLRP3$^{+/+}$ and KC;NLRP3$^{-/-}$ mice were sacrificed at 3, 6, or 9 mo of life (means of six to seven mice per time point). Representative H&E-stained sections are shown. The percentage of pancreatic area occupied by intact acinar structures and the fractions of ductal structures exhibiting normal morphology, acinoductal metaplasia (ADM), or graded pancreatic intraepithelial neoplasia (PanIN) I–III lesions were calculated. Bar, 200 µm. (B) Weights of pancreata were compared in 3- and 6-mo-old KC;NLRP3$^{+/+}$ and KC;NLRP3$^{-/-}$ mice. (C) Pancreata of 6-mo-old KC;NLRP3$^{+/+}$ and KC;NLRP3$^{-/-}$ mice were stained with trichrome, and the percentage of fibrotic pancreas' area was calculated. Bar, 200 µm. Unpaired Student's *t* test was used for statistical analyses. (D) Kaplan-Meier survival analysis was performed for KC;NLRP3$^{+/+}$ (n = 29) and KC;NLRP3$^{-/-}$ (n = 24) mice. P = 0.002 based on the Wilcoxon test. (E) WT and NLRP3$^{-/-}$ mice were challenged with orthotopically implanted KPC-derived tumor cells. Mice were sacrificed at 21 d, and pancreatic tumors were photographed and weighed. n = 8/group. Bar, 1 cm. Orthotopic tumor experiments were repeated more than five times with similar results. Unpaired Student's *t* test was used for statistical analyses. Mice were bred in house, and littermate controls were used. **, P < 0.01; ***, P < 0.001. Data are presented as mean ± standard error.

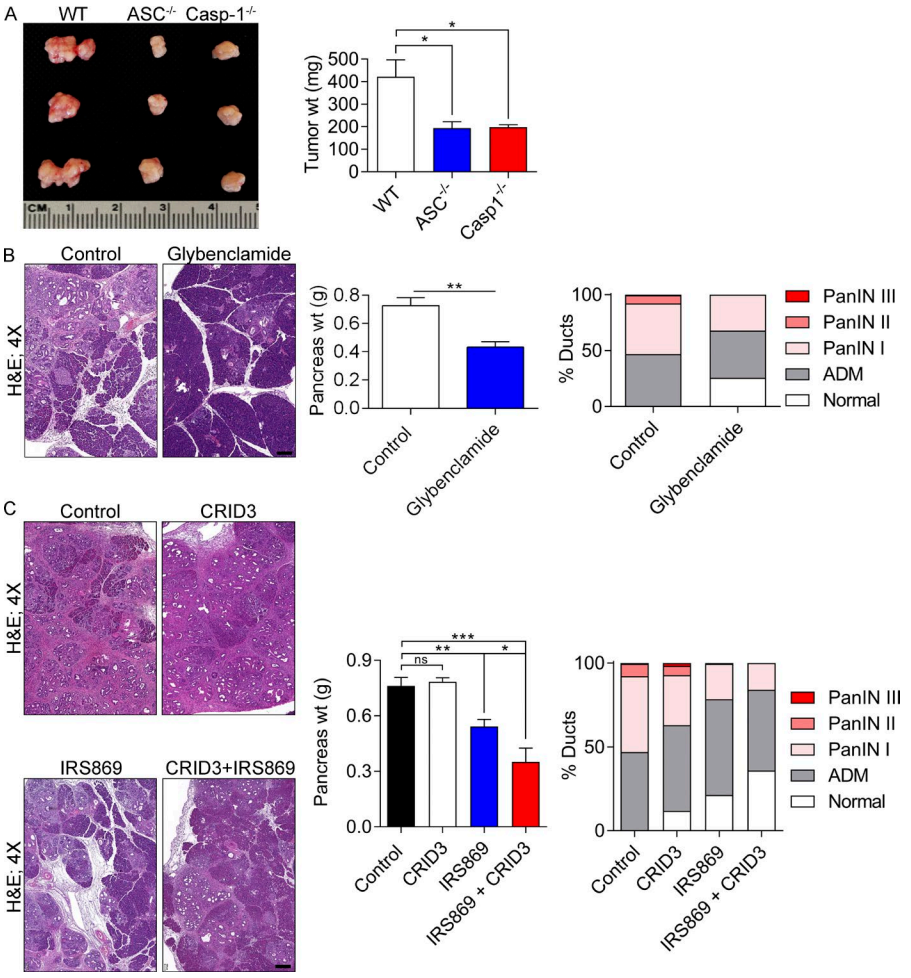

Figure 3. **ASC or caspase-1 deletion and NLRP3 inhibition are protective in murine disease.** (A) WT, ASC$^{-/-}$, and caspase-1$^{-/-}$ mice were orthotopically implanted with KPC-derived tumor cells. At 21 d, intrapancreatic tumors were harvested. Representative photographs of tumors and quantitative analysis of tumor weights are shown for each group. n = 5/group. (B) 6-wk-old KC mice were serially treated for 8 wk with Glybenclamide or vehicle before sacrifice. Pancreata were harvested, weighed, and analyzed for ductal dysplasia based on H&E staining. n = 5/group. Bar, 200 µm. (C) 6-wk-old KC mice were serially treated for 8 wk with vehicle, a TLR9 oligonucleotide inhibitor (IRS869), CRID3, or IRS869 + CRID3. Pancreata were harvested, weighed, and analyzed by H&E staining. n = 5/group. Bar, 200 µm. Littermate controls were used in all experiments, and experiments were reproduced twice. Unpaired Student's t test was used for statistical analyses. *, $P < 0.05$; **, $P < 0.01$; ***, $P < 0.001$. ADM, acinoductal metaplasia; PanIN, pancreatic intraepithelial neoplasia.

notype. Whereas PDA-infiltrating CD4$^+$ T cells exhibited prominent T reg, Th2, and Th17 cell differentiation in WT hosts—as evidenced by high expression of FoxP3, GATA-3, IL-10, and IL-17—NLRP3 deletion resulted in reduced CD4$^+$ T cell expression of these tumor-promoting transcription factors and cytokines (Fig. 7 B). Accordingly, NLRP3 deletion increased Tbet, IFN-γ, and TNF expression in PDA-infiltrating CD4$^+$ T cells, suggesting enhanced Th1 cell differentiation (Fig. 7 C). Similarly, NLRP3 deletion increased PDA-infiltrating CD8$^+$ T cell expression of T-bet and IFN-γ, indicative of cytotoxic T cell activation (Fig. 7 D). Furthermore, PDA-infiltrating CD4$^+$ and CD8$^+$ T cells each up-regulated CD44 and PD-1 expression but lowered CD62L in the context of NLRP3 deletion, consistent with an activated phenotype (Fig. 7, E–G). We recently reported that T cells are entirely dispensable in PDA, as T cell deletion does not influence PDA growth in WT hosts (Daley et al., 2016; Seifert et al., 2016a). Conversely, in vivo, CD4$^+$ or CD8$^+$ T cell deletion abrogated the protective effects of NLRP3 deletion (Fig. 7 H). Moreover, adoptive transfer of T cells from PDA-bearing NLRP3$^{-/-}$ mice protected against KPC tumor growth compared with transfer of tumor-entrained WT T cells (Fig. 7 I). These data confirm that interruption of NLRP3 signaling induces T cell–dependent antitumor immunity. Notably, we did not find evidence of enhanced T cell migration in NLRP3-deficient PDA using in vivo or in vitro models (Fig. S3). Furthermore, in contrast to targeting NLRP3, NOD2 deletion did not alter macrophage polarization or T cell differentiation within the PDA TME (Fig. 4, C–G).

Because we found that both IL-18 and IL-1β are up-regulated in PDA, we tested whether these were important mediators of tumorigenesis. IL-18 blockade did not influence PDA growth in WT or NLRP3$^{-/-}$ mice (Fig. S4 A). However, IL-1β blockade was protective against PDA in WT hosts but failed to further protect NLRP3$^{-/-}$ hosts, suggesting that IL-1β is protumorigenic in PDA in an NLRP3-dependent manner (Fig. S4 A). IL-1β blockade reversed the M2-like macrophage phenotype in vitro and in vivo in PDA (Fig. S4, B–D). Accordingly, IL-1β neutralization rescued the capacity of antigen-pulsed PDA-infiltrating NLRP3$^{+/+}$ TAMs to activate antigen-restricted T cells but had no effect in NLRP3$^{-/-}$ TAMs (Fig. S4, E and F).

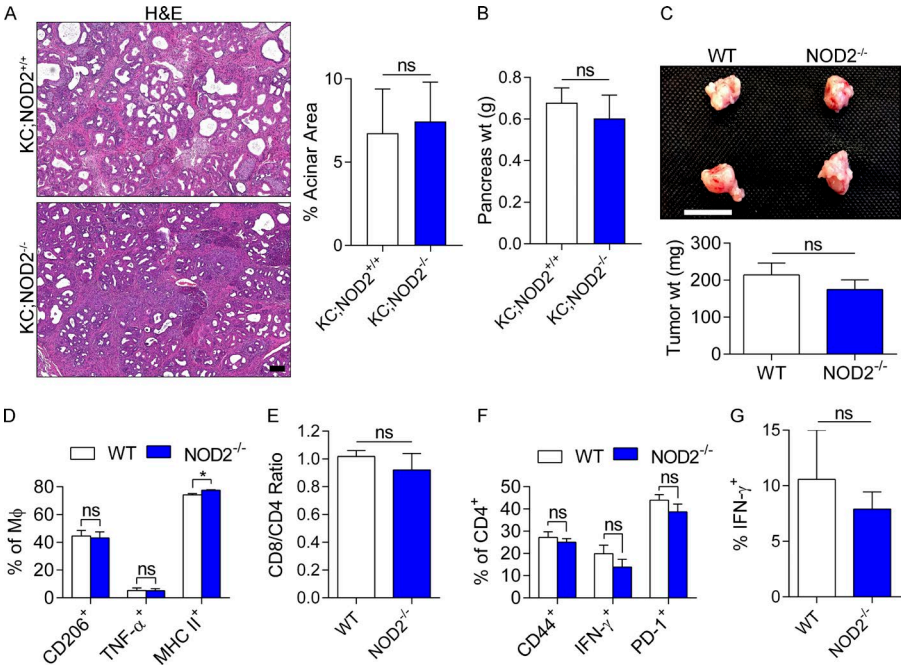

Figure 4. **NOD2 deletion is not protective against PDA.** (A and B) Cohorts of KC and KC;NOD2$^{-/-}$ mice were sacrificed at 6 mo of life. Mean n = 6/group. (A) Representative H&E-stained sections are shown, and the fraction of preserved acinar area was calculated (P = NS). Bar, 200 µm. (B) Pancreas weights (wt) were recorded (P = NS). (C–G) WT and NOD2$^{-/-}$ mice were orthotopically implanted with KPC-derived tumor cells. (C) Mice were sacrificed at 21 d. Representative gross pictures of tumors and mean tumor weights are shown (P = NS). n = 5/group. Bar, 1 cm. (D) Expression of CD206, TNF, and MHC II in TAMs were determined by flow cytometry. *, P < 0.05. MΦ, macrophage. (E–G) Similarly, the intratumoral CD8$^+$/CD4$^+$ T cell ratio (P = NS; E), CD4$^+$ T cell expression of CD44, IFN-γ, and PD-1 (F), and CD8$^+$ T cell expression of IFN-γ (G) were assessed (P = NS). Orthotopic tumor experiments in NOD2$^{-/-}$ mice were repeated four times with similar results, and littermate controls were used. Unpaired Student's t test was used for statistical analyses.

DISCUSSION

PDA is the third leading cause of cancer-related death in the US, and there are few promising new therapies on the horizon (Rahib et al., 2016). There are no effective means to prevent disease onset, and treatment options are extremely limited once transformation has occurred. Surgical resection is curative in ∼5% of PDA patients, and conventional chemotherapeutics offer only transient benefit. Ineffective development of an adaptive T cell immune response against PDA remains a potential bottleneck in extending patient survival. Macrophage infiltration has been associated with poor prognosis in human PDA (Di Caro et al., 2016). Furthermore, regulation of macrophage polarization is critical in T cell education in the TME. We recently reported that expansion of IL-10$^+$CD206$^+$ immune-suppressive M2-like TAMs, as a consequence of ionizing radiation or necroptotic cell death, results in the recruitment of tumor-promoting Th2 and T reg cells (Seifert et al., 2016a,b). Similarly, Th17 cells support oncogenesis, as IL-17 has direct mitogenic effects on transformed epithelial cells (McAllister et al., 2014). By contrast, Th1 cell polarization of CD4$^+$ T cells and CD8$^+$ T cell activation are associated with enhanced antitumor immunity in mouse models of PDA and extended survival in human disease (De Monte et al., 2011). A critical finding in the current work is that NLRP3 signaling in macrophages governs the polarization of TAMs and, hence, controls the keys to immunogenic or tolerogenic CD4$^+$ T cell differentiation and CD8$^+$ T cell activation. We found that IL-10 or IL-1β blockade reversed the tolerogenic influences of NLRP3$^{+/+}$ TAMs but did not enhance the immunogenic function of NLRP3$^{-/-}$ TAMs, which express minimal IL-10 and IL-1β. Notably, in addition to promoting adaptive immune suppression, IL-10 expression in PDA-associated macrophages has been shown to drive epithelial–mesenchymal transition in pancreatic cancer cells (Liu et al., 2013). In addition, obesity has recently been shown to promote PDA growth and resistance to chemotherapy via IL-1β expression from both peripancreatic adipocytes and PSCs, which in turn recruit neutrophils and induce fibrosis (Incio et al., 2016). However, we did not appreciate NLRP3 expression in PSCs. Similarly, NLRP3 signaling in TAMs did not differentially influence their capacity for PSC activation, suggesting an alternative mechanism.

T cell checkpoint receptor-based immunotherapy regimens have failed to show efficacy in early clinical trials in PDA (Kunk et al., 2016). The apparent futility of checkpoint receptor- or ligand-targeted approaches in PDA suggests that complementary adjuvants may be necessary to achieve antitumor immunity. For example, recent work suggested that targeting CXCR2, which reduces immune-suppressive myeloid cell recruitment, enables efficacy for PD-1 targeted therapy (Steele et al., 2016). Of note, our work demonstrates that PD-1 is expressed at minimal levels in CD4$^+$ and CD8$^+$ T cells in PDA at baseline, but PD-1 is markedly up-regulated by interruption of NLRP3 signaling. These data are consistent with the higher expression of checkpoint receptors in activated T cells (Pardoll, 2012). Hence, our findings suggest that combining NLRP3 + checkpoint-targeted therapies may offer synergistic benefit, as interrupting NLRP3 will activate CD4$^+$ and CD8$^+$ T cells via repolarization of TAMs; concomitantly, PD-1 blockade may mitigate the potential for checkpoint receptor-mediated rebound immune suppression resulting from elevated PD-1 expression.

We have previously reported that selective ligation or deletion of innate immune receptors or their associated adap-

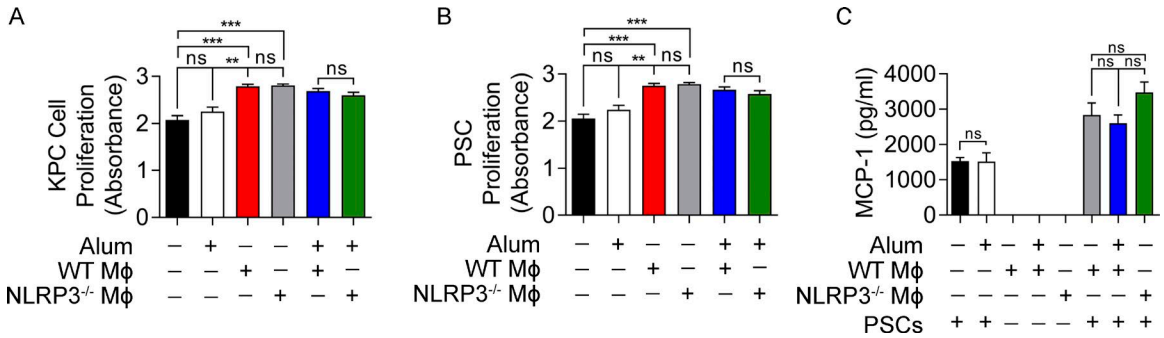

Figure 5. **NLRP3 signaling does not enable TAMs to directly induce tumor cell proliferation or PSC activation.** (A) KPC tumor cells were cultured alone or with the NLRP3 agonist alum, WT macrophages, or NLRP3$^{-/-}$ macrophages FACS sorted from orthotopic PDA tumors, in single or in the indicated combinations. Tumor cell proliferation was measured using the XTT assay. (B and C) PSCs were cultured alone or with the NLRP3 agonist alum, WT macrophages, or NLRP3$^{-/-}$ macrophages, in single or in the indicated combinations. (B) PSC proliferation was measured using the XTT assay. (C) MCP-1 was measured in the cell culture supernatant. All experiments were performed in replicates of five and repeated twice with similar results. Unpaired Student's *t* test was used for statistical analyses. **, P < 0.01; ***, P < 0.001. Data are presented as mean ± standard error. MΦ, macrophage.

tor proteins can have divergent influences on oncogenesis in PDA. For example, ligation of TLR7 promotes tumorigenesis via activation of NF-κB, MAPK, and notch-dependent signaling mechanisms (Ochi et al., 2012a). TLR9 signaling in PSCs accentuates peritumoral fibrosis and results in the secretion of protumorigenic cytokines and chemokines leading to the recruitment of myeloid-derived suppressor cells (Zambirinis et al., 2015). Interestingly, we found that blockade of TLR9 and NLRP3 had synergistic protective effects in KC mice. Similarly, in benign pancreatic disease, TLR9 and NLRP3 signaling reportedly cooperate to promote edema and inflammation in acute pancreatitis (Hoque et al., 2011). TLR signaling is a required priming step for NLRP3 signaling (Latz et al., 2013). It is conceivable that TLR9 synergizes with the NLRP3 inhibition, as dual inhibition will block both the production of pro–IL-1β and the activation of IL-1β. In contrast to these findings, blockade of Myd88, an adaptor protein common to most TLR-dependent pathways, accelerated pancreatic tumorigenesis by directing DCs toward induction of immune-suppressive Th2 CD4$^+$ cells (Ochi et al., 2012b). Besides TLRs, perturbation of other families of pattern recognition receptors within the pancreas also influences tumorigenesis. For example, ligation of the C-type lectin receptor Mincle by byproducts of necroptotic cell death results in the expansion of immune-suppressive myeloid cells, leading to corrupted adaptive immunity and accelerated tumor growth (Seifert et al., 2016a).

Our findings that NLRP3 signaling promotes PDA progression contrasts with its role in other gastrointestinal cancers. In gastric carcinoma, deletion of IL-18, ASC, and caspase-1 have each been associated with accelerated tumorigenesis (Allen et al., 2010; Dupaul-Chicoine et al., 2010; Salcedo et al., 2010; Zaki et al., 2010). Similarly, in colon adenocarcinoma, deletion of components of the inflammasome is associated with more aggressive tumor growth, as the inflammasome is thought to be required for robust NK cell tumoricidal activity (Elinav et al., 2011; Hu et al., 2011). Although our findings in PDA are seemingly contrary with these studies, the patterns are not necessarily paradoxical, as the effects of NLRP3 activation in neoplastic progression may be contingent on the differential roles played by immunity and inflammation in each specific malignancy (Karki et al., 2017). In particular, in malignant processes without a driving inflammatory component, NLRP3 signaling may enable antigen-presenting cells to overcome immunological tolerance, promoting antitumor immune responses. However, in neoplastic conditions, such as PDA, that arise from chronic inflammation and are driven by ongoing inflammation associated with immune-suppressive CD4$^+$ T cells (Demols et al., 2000; Ochi et al., 2012b), selective NLRP3 ligation may sustain this protumorigenic inflammatory state.

The notion that PDA invariably arises from inflammatory disease is supported by both experimental evidence and clinical observations. For example, Guerra et al. (2007) reported that a driving oncogenic *Kras* mutation is insufficient to induce PDA progression unless mice experience concomitant chronic pancreatitis. Furthermore, patients suffering from chronic pancreatitis have an eightfold-increased risk of PDA development, and familial pancreatitis is associated with a 40–75% lifetime risk of pancreatic neoplasia (Lowenfels et al., 1993, 1997). It is interesting that deletion of the NOD2 inflammasome did not affect tumorigenesis. However, unlike NLRP3 signaling, we found that NOD2 signaling does not influence intratumoral macrophage polarization and, consequently, does not affect the terminal differentiation of CD4$^+$ T cells or CD8$^+$ T cell activation within the PDA TME. In summary, our data suggest that NLRP3 is an attractive novel target for experimental therapeutics with the goal of reprogramming the TME toward an immunogenic innate and adaptive inflammatory phenotype.

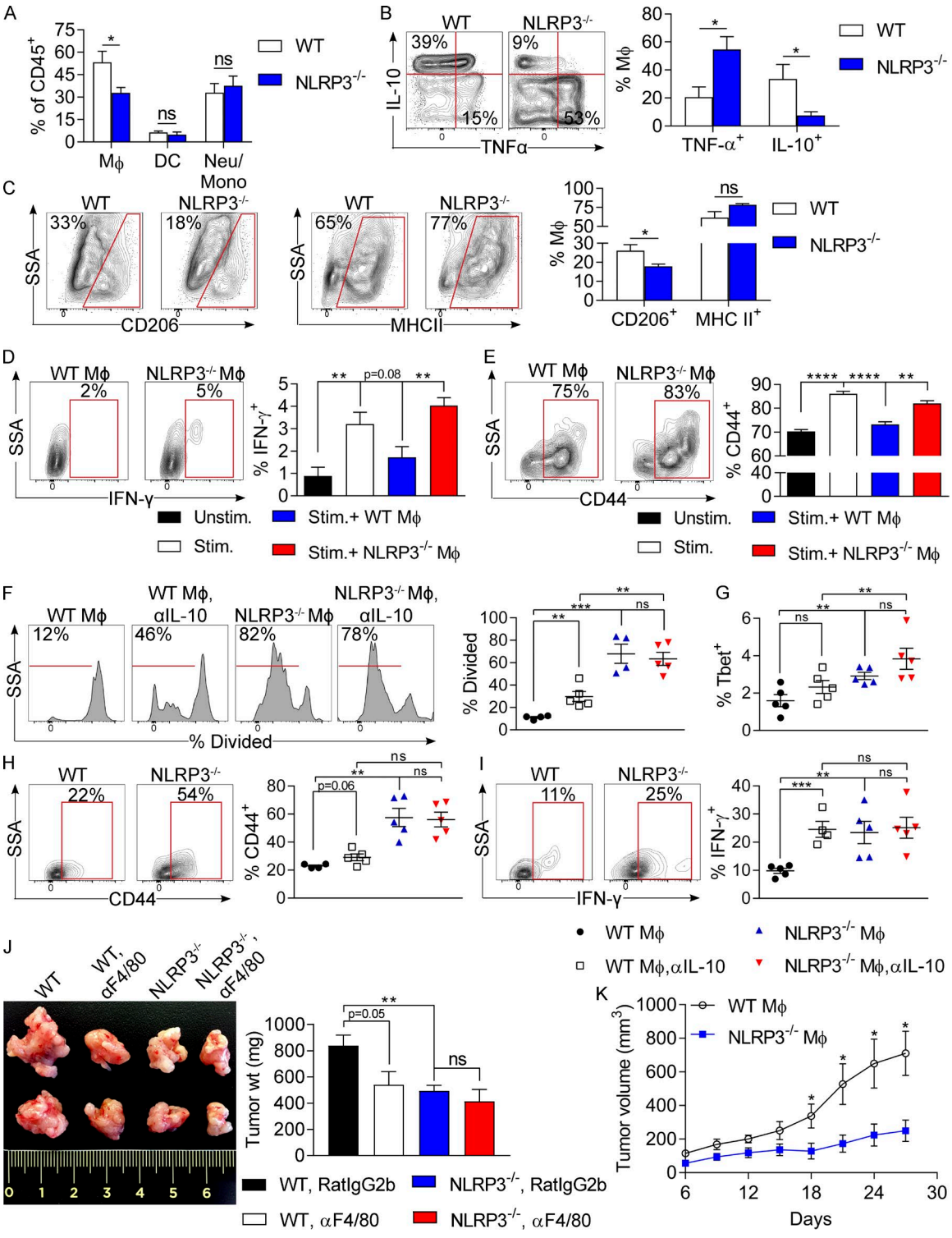

Figure 6. **NLRP3 deletion induces immunogenic reprogramming of TAMs.** (A) WT and NLRP3$^{-/-}$ mice were orthotopically implanted with KPC-derived tumor cells. Tumors were harvested at 3 wk. The fraction of tumor-infiltrating Gr1^{-}CD11c^{-}CD11b^{+}F4/80^{+} macrophages, CD11c^{+}MHCII^{+}F4/80^{-} DCs, and Gr1^{+}CD11b^{+} neutrophils and inflammatory monocytes were determined by flow cytometry. (B and C) PDA-infiltrating macrophages in WT and NLRP3$^{-/-}$ hosts were gated and tested for expression of TNF and IL-10 (B) and CD206 and MHC II (C). Experiments were reproduced greater than three times using five mice per group. (D and E) Splenic CD8^{+} T cells from untreated WT mice were cultured in 96-well plates, either unstimulated or stimulated with αCD3/αCD28 alone or in co-culture with PDA-infiltrating WT or NLRP3$^{-/-}$ TAMs. CD8^{+} T cell expression of IFN-γ (D) and CD44 (E) were determined at 72 h by flow cytometry. (F–I) TAMs were harvested from orthotopic KPC tumors in WT and NLRP3$^{-/-}$ hosts, pulsed with OVA$_{257–264}$ peptide, and plated with CFSE-labeled CD8^{+} OT-I T

MATERIALS AND METHODS

Animals and in vivo models

C57BL/6 (H-2Kb), OT-I, OT-II, NOD2$^{-/-}$, and Casp1$^{-/-}$ mice were purchased from The Jackson Laboratory. NLRP3$^{-/-}$ mice were a gift from G. Nunez (University of Michigan, Ann Arbor, MI). ASC$^{-/-}$ mice were obtained from Genentech. KC mice were a gift from D. Bar-Sagi (New York University, New York, NY), and data regarding these mice were previously described by us (Daley et al., 2016; Seifert et al., 2016a). All mice were bred in house for a minimum of eight generations before use in experiments. For orthotopic pancreatic tumor challenge, mice were administered intrapancreatic injections of FC1242 tumor cells derived from KPC mice using methods we previously described (Zambirinis et al., 2015). In preparation for intrapancreatic injection, cells were suspended in PBS with 50% Matrigel (BD) at 10^6 cells/ml, and 10^5 cells were injected into the body of the pancreas via laparotomy. Mice were sacrificed 3 wk later, and tumor weight was recorded. In some experiments, mice were serially administered an oligonucleotide inhibitor of TLR9 (IRS869; 84.8 µg/d, i.p.; Enzo Life Sciences), CRID3 (800 µg/d, i.p.; gift from L. O'Neill, Trinity College, Dublin, Ireland), or Glybenclamide (1 mg/d, i.p.; InvivoGen) for 8 wk. In select experiments, TGF-β (1D11.16.8), IL-1β (B122), IL-18 (YIG1F74-1G7), CD4 T cells (GK1.5), CD8 T cells (53-6.72), and macrophages (F4/80; CI:A3-1; all Bio X Cell) were neutralized using mAb regimens we have previously described (Daley et al., 2016; Seifert et al., 2016a). In other experiments, 10^6 KPC-derived tumor cells were administered subcutaneously, alone or mixed with 4×10^4 tumor-entrained macrophages or 2×10^4 T cells. All animal procedures were approved by the New York University School of Medicine Institutional Animal Care and Use Committee.

Cellular harvest and flow cytometry

Human or mouse single-cell suspensions were prepared as described previously with slight modifications (Ochi et al., 2012b). Briefly, pancreata were placed in cold RPMI 1640 medium with 1 mg/ml collagenase IV (Worthington Biochemical Corporation) and 2 U/ml DNase I (Promega) and minced with scissors to submillimeter pieces. Then, tissues were incubated at 37°C for 30 min with gentle shaking every 5 min. Specimens were passed through a 70-µm mesh and centrifuged at 350 *g* for 5 min. PSCs were further enriched and propagated as previously detailed (Zambirinis et al., 2015). For flow cytometry experiments, the cell pellet was resuspended in cold PBS with 1% FBS. After blocking FcγRIII/II with an anti-CD16/CD32 mAb (eBioscience), cell labeling was performed by incubating 10^6 cells with 1 µg of fluorescently conjugated mAbs directed against mouse CD44 (IM7), CD62L (MEL-14), IL-17 (TC11-18H10.1), CD25 (3C7), CD206 (C068C2), PD-1 (29F.1A12), CD3 (17A2), CD4 (RM4-5), CD8 (53-6.7), CD45 (30-F11), CD11b (M1/70), CD80 (16-10A1), CD86 (GL-1), CD11c (N418), Gr1 (RB6-8C5), LFA-1 (H155-78), MHC II (M5/114.15.2), IL-10 (JES5-16E3), IFN-γ (XMG1.2), TNF (MP6-XT22; all BioLegend), T-bet (eBio4B10), GATA-3 (TWAJ), FoxP3 (FJK-16s; all eBioscience), CCR2 (REA538; Miltenyi Biotec), NLRP3 (768319), and IL-1β (166931; both R&D Systems). Human pancreas and PBMCs were costained with mAbs directed against CD45 (HI30), CD15 (W6D3; both BioLegend), and NLRP3 (768319; R&D Systems). Intracellular staining for cytokines and transcription factors was performed using the Fixation-Permeabilization Solution kit (BD). Flow cytometry was performed on an LSRII flow cytometer (BD). Data were analyzed using FlowJo (v.10.1; Tree Star). Human tissues were obtained under an institutional review board–approved protocol.

In vitro experiments

FACS-purified macrophages were co-cultured with KPC-derived tumor cells or PSCs in a 1:5 ratio for 24 h, unless otherwise specified. In select experiments, 200 µg/ml of the NLRP3 agonist alum (InvivoGen) was added to co-culture wells. No additional growth factors were added. Tumor cell or PSC proliferation was measured using the XTT assay kit according to the manufacturer's protocol (Sigma-Aldrich). Cytokine levels in cell culture supernatants were determined in a cytometric bead array (BD). BMDMs were generated as previously described (Greco et al., 2016). In some experiments, day-10 BMDMs were treated with 8 pg/ml of recombinant mouse TNF (Cell Signaling Technology) or 0.2 ng/ml TGF-β (R&D Systems) for 18 h before analysis for NLRP3 expression by flow cytometry. For antibody-based T cell stimulation assays, splenic CD8$^+$ T cells were activated using CD3/CD28 coligation in 96-well plates as we previously described (Daley et al., 2016). In selected wells, PDA-infiltrating macrophages were added in a 1:5 macrophage/T cell ratio. T cell activation was analyzed at 72 h. For antigen-restricted T cell stimulation assays, CFSE-labeled OT-I or OT-II T cells were cultured with, respectively, $OVA_{257–264}$- or $OVA_{323–339}$-pulsed TAMs in a 5:1 ratio. In select experiments, a neutralizing IL-1β (B122) or IL-10 mAb (JES5-2A5; all Bio X Cell) or isotype control

cells. (F) T cell proliferation at 96 h was determined by dilution of CFSE. (G–I) T-bet (G), CD44 (H), and IFN-γ (I) expression in the CD8$^+$ T cells was assessed by flow cytometry. Experiments were performed using five biological replicates per group and repeated twice. Unpaired Student's *t* test was used for statistical analyses. (J) WT and NLRP3$^{-/-}$ mice were orthotopically implanted with KPC-derived tumor cells and serially treated with neutralizing αF4/80 mAb or isotype control. Cohorts of mice were sacrificed on day 21. Representative images and quantitative data on tumor weights are shown. *n* = 5/group. Unpaired Student's *t* test was used for statistical analyses. (K) Littermate NLRP3$^{-/-}$ mice were subcutaneously implanted with KPC-derived PDA tumor cells admixed with tumor-entrained WT or NLRP3$^{-/-}$ macrophages. Tumor volume was recorded at serial intervals. Adoptive transfer experiments were repeated twice. *n* = 5/group. Unpaired Student's *t*-test was used for statistical analyses. *, P < 0.05; **, P < 0.01; ***, P < 0.001; ****, P < 0.0001. Data are presented as mean ± standard error. Mono, monocyte; Neu, neutrophil; SSA, side scatter; Stim., stimulated; Unstim., unstimulated; wt, weight.

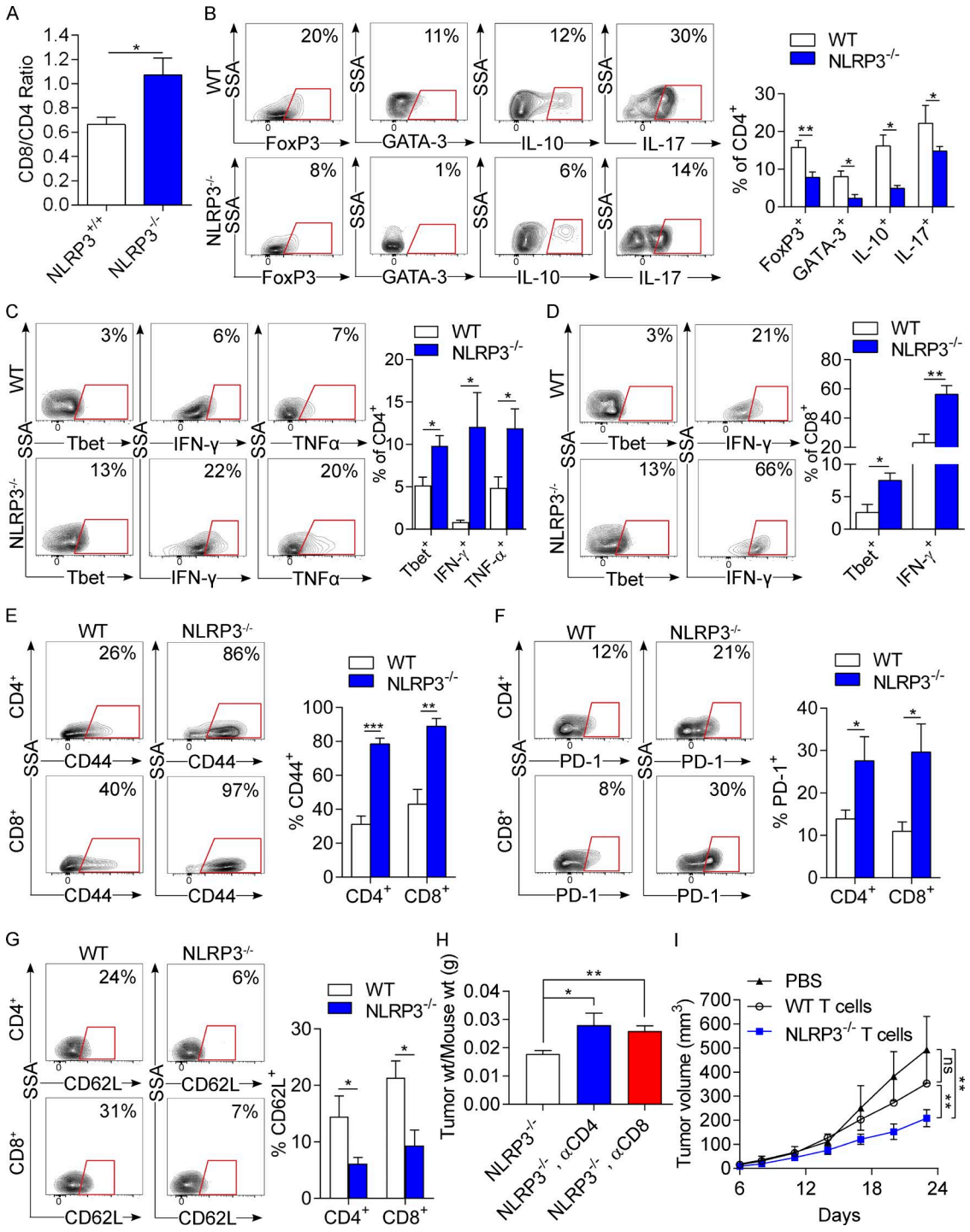

Figure 7. **NLRP3 deletion results in immunogenic T cell differentiation in PDA.** (A–G) WT and NLRP3$^{-/-}$ mice were orthotopically implanted with KPC-derived tumor cells. Tumors were harvested at 3 wk, and single-cell suspensions were analyzed by flow cytometry. (A) The CD8$^+$/CD4$^+$ T cell ratio was calculated. (B) Tumor-infiltrating CD4$^+$ T cells were gated and tested for expression of FoxP3, GATA-3, IL-10, and IL-17. (C) CD4$^+$ T cells were also tested for T-bet, IFN-γ, and TNF expression. (D) CD8$^+$ T cells were gated and tested for expression of T-bet and IFN-γ. (E–F) Intratumoral CD4$^+$ and CD8$^+$ T cells were analyzed for expression of CD44 (E), PD-1 (F), and CD62L (G). Each experiment was repeated more than three times, using at least four mice per group. Representative contour plots and quantitative data are shown. Unpaired Student's *t* test was used for statistical analyses. (H) Cohorts of littermate NLRP3$^{-/-}$ animals serially treated with neutralizing αCD4 or αCD8 mAbs or isotype were challenged with orthotopic PDA. Mice were sacrificed at 21 d, and pancreatic tumors were weighed. (I) Littermate WT mice were subcutaneously implanted with KPC-derived PDA tumor cells alone or admixed with tumor-entrained CD3$^+$ WT or NLRP3$^{-/-}$ T cells. Tumor volume was recorded at serial intervals. T cell depletion and T cell adoptive transfer experiments were repeated twice. n = 5/group. Unpaired Student's *t* test was used for statistical analyses. *, $P < 0.05$; **, $P < 0.01$; ***, $P < 0.001$. Data are presented as mean ± standard error. SSA, side scatter; wt, weight.

was used. In other experiments, OT-II splenocytes were cultured directly with $OVA_{323–339}$ peptide, either alone or in the presence of tumor-infiltrating $Gr1^+CD11b^+$ cells (10:1 ratio) as we previously described (Daley et al., 2016). T cell activation was determined at 96 h by flow cytometry.

T cell migration experiments

To evaluate T cell migration in vivo, day-18 PDA-bearing mice were administered 10^6 $CD45.1^+$ T cells via retroorbital injection. The number of PDA-infiltrating $CD45.1^+$ T cells was determined at 36 h by flow cytometry. To evaluate T cell migration in vitro, we use QCM Chemotaxis Cell Migration Assay (EMD Millipore). $CD3^+$ T cells were harvested from WT or $NLRP3^{-/-}$ hosts and starved overnight. 5×10^5 $CD3^+$ T cells were added to a 3-µm insert over a lower chamber in a 24-well dish in the presence or absence of 10% FBS for 18 h. Cellular migration was measured using colorimetric parameters as per the manufacturer's instructions.

Western blotting

For protein extraction from tissues, 15–30 mg of human or mouse pancreatic tissue was homogenized in 150–300 µl (i.e., 10 times the weight) of ice-cold radioimmunoprecipitation assay buffer. Total protein was quantified using the DC Protein Assay according to the manufacturer's instructions (Bio-Rad Laboratories). Western blotting was performed as previously described with minor modifications (Ochi et al., 2012b). In brief, 10% Bis-Tris polyacrylamide gels (NuPage; Invitrogen) were equiloaded with 10–30 µg of protein, electrophoresed at 200 V, and electrotransferred to polyvinylidene fluoride membranes. After blocking with 5% BSA, membranes were probed with primary antibodies to IL-1β (3A6; Cell Signaling Technology) and IL-18 (ab71495; Abcam). Blots were developed by enhanced chemilumescent (Thermo Fisher Scientific).

Histology, immunohistochemistry, and microscopy

For histological analysis, pancreatic specimens were fixed with 10% buffered formalin, dehydrated in ethanol, embedded with paraffin, and stained with hematoxylin and eosin (H&E) or Gomori's Trichrome. The fraction of preserved acinar area was calculated as previously described (Daley et al., 2016). Pancreatic ductal dysplasia was graded according to established criteria (Hruban et al., 2001). Immunofluorescent staining in frozen mouse tissues was performed using antibodies against CD11b (M1/70; BioLegend), CK19 (Troma-III; Developmental Studies Hybridoma Bank), NLRP3 (768319; R&D Systems), and DAPI (Vector Laboratories). For analysis of human tissues, de-identified paraffin-embedded PDA specimens were probed with an mAb directed against NLRP3 (768319; R&D Systems). All human tissues were collected using an institutional review board–approved protocol. Quantifications were performed by assessing 10 high-power fields (40×) per slide. Immunofluorescent images were acquired using a confocal microscope (LSM700; ZEISS) with ZEN 2010 software (ZEISS).

Statistical analysis

Data are presented as mean ± standard error. Survival was measured according to the Kaplan-Meier method. Statistical significance was determined by Student's *t* test and Wilcoxon test using Prism 7 (GraphPad Software). P-values <0.05 were considered significant.

Online supplemental material

Fig. S1 shows that adoptive transfer of tumor-entrained $NLRP3^{-/-}$ macrophages enhances intratumoral T cell activation. Fig. S2 shows the phenotype and T cell inhibitory effects of PDA-infiltrating neutrophils and inflammatory monocytes in the context of NLRP3 deletion. Fig. S3 shows that T cells do not exhibit increased migration in PDA in $NLRP3^{-/-}$ hosts. Fig. S4 shows IL-1β blockade protects against PDA and enhances the capacity of TAMs to activate T cells.

ACKNOWLEDGMENTS

This work was supported by National Institutes of Health grants (CA168611, CA155649, and CA206105 to G. Miller), the Department of Defense Peer Reviewed Medical Research Program (G. Miller), the Lustgarten Foundation (G. Miller), the American Association for Cancer Research Pancreatic Cancer Action Network (G. Miller), the Hirshberg Foundation for Pancreatic Cancer Research (G. Miller), and the Irene and Bernard Schwartz Fellowship in Gastrointestinal Oncology (D. Daley).

The authors declare no competing financial interests.

Author contributions: D. Daley and V.R. Mani: project leadership, data collection, and data analysis; N. Mohan: flow cytometry, Western blotting, in vivo experiments, and manuscript preparation; N. Akkad: immunohistochemistry, immunofluorescence, flow cytometry, and in vivo experiments; G.S.D. Balasubramania Pandian, S. Savadkar, and K.B. Lee: flow cytometry and in vivo experiments; A. Torres-Hernandez, B. Aykut, B. Diskin, and W. Wang: technical assistance; G. Werba: Western blotting and manuscript preparation; M.S. Farooq, A.I. Mahmud, E.J. Morales, S. Lall, B.J. Wadowski, A.G. Rubin, M.E. Berman, and R. Narayanan: data collection; M. Hundeyin: technical assistance and data analysis; and G. Miller: project design, data analysis, and manuscript preparation.

Submitted: 7 October 2016
Revised: 10 February 2017
Accepted: 14 March 2017

REFERENCES

Allen, I.C., E.M. TeKippe, R.M. Woodford, J.M. Uronis, E.K. Holl, A.B. Rogers, H.H. Herfarth, C. Jobin, and J.P. Ting. 2010. The NLRP3 inflammasome functions as a negative regulator of tumorigenesis during colitis-associated cancer. *J. Exp. Med.* 207:1045–1056. http://dx.doi.org/10.1084/jem.20100050

Clark, C.E., S.R. Hingorani, R. Mick, C. Combs, D.A. Tuveson, and R.H. Vonderheide. 2007. Dynamics of the immune reaction to pancreatic cancer from inception to invasion. *Cancer Res.* 67:9518–9527. http://dx.doi.org/10.1158/0008-5472.CAN-07-0175

Coll, R.C., A. Robertson, M. Butler, M. Cooper, and L.A. O'Neill. 2011. The cytokine release inhibitory drug CRID3 targets ASC oligomerisation in the NLRP3 and AIM2 inflammasomes. *PLoS One.* 6:e29539. http://dx.doi.org/10.1371/journal.pone.0029539

Daley, D., C.P. Zambirinis, L. Seifert, N. Akkad, N. Mohan, G. Werba, R. Barilla, A. Torres-Hernandez, M. Hundeyin, V.R. Mani, et al. 2016. γδ T cells support pancreatic oncogenesis by restraining αβ T cell activation. *Cell.* 166:1485–1499.e15. http://dx.doi.org/10.1016/j.cell.2016.07.046

Demols, A., O. Le Moine, F. Desalle, E. Quertinmont, J.L. Van Laethem, and J. Devière. 2000. $CD4^+$ T cells play an important role in acute experimental pancreatitis in mice. *Gastroenterology.* 118:582–590. http://dx.doi.org/10.1016/S0016-5085(00)70265-4

De Monte, L., M. Reni, E. Tassi, D. Clavenna, I. Papa, H. Recalde, M. Braga, V. Di Carlo, C. Doglioni, and M.P. Protti. 2011. Intratumor T helper type 2 cell infiltrate correlates with cancer-associated fibroblast thymic stromal lymphopoietin production and reduced survival in pancreatic cancer. *J. Exp. Med.* 208:469–478. http://dx.doi.org/10.1084/jem.20101876

Di Caro, G., N. Cortese, G.F. Castino, F. Grizzi, F. Gavazzi, C. Ridolfi, G. Capretti, R. Mineri, J. Todoric, A. Zerbi, et al. 2016. Dual prognostic significance of tumour-associated macrophages in human pancreatic adenocarcinoma treated or untreated with chemotherapy. *Gut.* 65:1710–1720. http://dx.doi.org/10.1136/gutjnl-2015-309193

Dupaul-Chicoine, J., G. Yeretssian, K. Doiron, K.S. Bergstrom, C.R. McIntire, P.M. LeBlanc, C. Meunier, C. Turbide, P. Gros, N. Beauchemin, et al. 2010. Control of intestinal homeostasis, colitis, and colitis-associated colorectal cancer by the inflammatory caspases. *Immunity.* 32:367–378. http://dx.doi.org/10.1016/j.immuni.2010.02.012

Elinav, E., T. Strowig, A.L. Kau, J. Henao-Mejia, C.A. Thaiss, C.J. Booth, D.R. Peaper, J. Bertin, S.C. Eisenbarth, J.I. Gordon, and R.A. Flavell. 2011. NLRP6 inflammasome regulates colonic microbial ecology and risk for colitis. *Cell.* 145:745–757. http://dx.doi.org/10.1016/j.cell.2011.04.022

Fowler, B.J., B.D. Gelfand, Y. Kim, N. Kerur, V. Tarallo, Y. Hirano, S. Amarnath, D.H. Fowler, M. Radwan, M.T. Young, et al. 2014. Nucleoside reverse transcriptase inhibitors possess intrinsic anti-inflammatory activity. *Science.* 346:1000–1003. http://dx.doi.org/10.1126/science.1261754

Fukunaga, A., M. Miyamoto, Y. Cho, S. Murakami, Y. Kawarada, T. Oshikiri, K. Kato, T. Kurokawa, M. Suzuoki, Y. Nakakubo, et al. 2004. CD8+ tumor-infiltrating lymphocytes together with CD4+ tumor-infiltrating lymphocytes and dendritic cells improve the prognosis of patients with pancreatic adenocarcinoma. *Pancreas.* 28:e26–e31. http://dx.doi.org/10.1097/00006676-200401000-00023

Greco, S.H., L. Tomkötter, A.K. Vahle, R. Rokosh, A. Avanzi, S.K. Mahmood, M. Deutsch, S. Alothman, D. Alqunaibit, A. Ochi, et al. 2015. TGF-β blockade reduces mortality and metabolic changes in a validated murine model of pancreatic cancer cachexia. *PLoS One.* 10:e0132786. http://dx.doi.org/10.1371/journal.pone.0132786

Greco, S.H., S.K. Mahmood, A.K. Vahle, A. Ochi, J. Batel, M. Deutsch, R. Barilla, L. Seifert, H.L. Pachter, D. Daley, et al. 2016. Mincle suppresses Toll-like receptor 4 activation. *J. Leukoc. Biol.* 100:185–194. http://dx.doi.org/10.1189/jlb.3A0515-185R

Guerra, C., A.J. Schuhmacher, M. Cañamero, P.J. Grippo, L. Verdaguer, L. Pérez-Gallego, P. Dubus, E.P. Sandgren, and M. Barbacid. 2007. Chronic pancreatitis is essential for induction of pancreatic ductal adenocarcinoma by K-Ras oncogenes in adult mice. *Cancer Cell.* 11:291–302. http://dx.doi.org/10.1016/j.ccr.2007.01.012

Hingorani, S.R., E.F. Petricoin, A. Maitra, V. Rajapakse, C. King, M.A. Jacobetz, S. Ross, T.P. Conrads, T.D. Veenstra, B.A. Hitt, et al. 2003. Preinvasive and invasive ductal pancreatic cancer and its early detection in the mouse. *Cancer Cell.* 4:437–450. http://dx.doi.org/10.1016/S1535-6108(03)00309-X

Hingorani, S.R., L. Wang, A.S. Multani, C. Combs, T.B. Deramaudt, R.H. Hruban, A.K. Rustgi, S. Chang, and D.A. Tuveson. 2005. Trp53R172H and KrasG12D cooperate to promote chromosomal instability and widely metastatic pancreatic ductal adenocarcinoma in mice. *Cancer Cell.* 7:469–483. http://dx.doi.org/10.1016/j.ccr.2005.04.023

Hiraoka, N., K. Onozato, T. Kosuge, and S. Hirohashi. 2006. Prevalence of $FOXP3^+$ regulatory T cells increases during the progression of pancreatic ductal adenocarcinoma and its premalignant lesions. *Clin. Cancer Res.* 12:5423–5434. http://dx.doi.org/10.1158/1078-0432.CCR-06-0369

Hoque, R., M. Sohail, A. Malik, S. Sarwar, Y. Luo, A. Shah, F. Barrat, R. Flavell, F. Gorelick, S. Husain, and W. Mehal. 2011. TLR9 and the NLRP3 inflammasome link acinar cell death with inflammation in acute pancreatitis. *Gastroenterology.* 141:358–369. http://dx.doi.org/10.1053/j.gastro.2011.03.041

Hruban, R.H., N.V. Adsay, J. Albores-Saavedra, C. Compton, E.S. Garrett, S.N. Goodman, S.E. Kern, D.S. Klimstra, G. Klöppel, D.S. Longnecker, et al. 2001. Pancreatic intraepithelial neoplasia: a new nomenclature and classification system for pancreatic duct lesions. *Am. J. Surg. Pathol.* 25:579–586. http://dx.doi.org/10.1097/00000478-200105000-00003

Hu, B., E. Elinav, and R.A. Flavell. 2011. Inflammasome-mediated suppression of inflammation-induced colorectal cancer progression is mediated by direct regulation of epithelial cell proliferation. *Cell Cycle.* 10:1936–1939. http://dx.doi.org/10.4161/cc.10.12.16008

Incio, J., H. Liu, P. Suboj, S.M. Chin, I.X. Chen, M. Pinter, M.R. Ng, H.T. Nia, J. Grahovac, S. Kao, et al. 2016. Obesity-induced inflammation and desmoplasia promote pancreatic cancer progression and resistance to chemotherapy. *Cancer Discov.* 6:852–869. http://dx.doi.org/10.1158/2159-8290.CD-15-1177

Karki, R., S.M. Man, and T.D. Kanneganti. 2017. Inflammasomes and cancer. *Cancer Immunol. Res.* 5:94–99. http://dx.doi.org/10.1158/2326-6066.CIR-16-0269

Kobayashi, M., F. Usui, T. Karasawa, A. Kawashima, H. Kimura, Y. Mizushina, K. Shirasuna, H. Mizukami, T. Kasahara, N. Hasebe, and M. Takahashi. 2016. NLRP3 deficiency reduces macrophage interleukin-10 production and enhances the susceptibility to doxorubicin-induced cardiotoxicity. *Sci. Rep.* 6:26489. http://dx.doi.org/10.1038/srep26489

Komada, T., F. Usui, A. Kawashima, H. Kimura, T. Karasawa, Y. Inoue, M. Kobayashi, Y. Mizushina, T. Kasahara, S. Taniguchi, et al. 2015. Role of NLRP3 inflammasomes for rhabdomyolysis-induced acute kidney injury. *Sci. Rep.* 5:10901. http://dx.doi.org/10.1038/srep10901

Kunk, P.R., T.W. Bauer, C.L. Slingluff, and O.E. Rahma. 2016. From bench to bedside a comprehensive review of pancreatic cancer immunotherapy. *J. Immunother. Cancer.* 4:14. http://dx.doi.org/10.1186/s40425-016-0119-z

Lamkanfi, M., J.L. Mueller, A.C. Vitari, S. Misaghi, A. Fedorova, K. Deshayes, W.P. Lee, H.M. Hoffman, and V.M. Dixit. 2009. Glyburide inhibits the Cryopyrin/Nalp3 inflammasome. *J. Cell Biol.* 187:61–70. http://dx.doi.org/10.1083/jcb.200903124

Latz, E., T.S. Xiao, and A. Stutz. 2013. Activation and regulation of the inflammasomes. *Nat. Rev. Immunol.* 13:397–411. http://dx.doi.org/10.1038/nri3452

Liu, C.Y., J.Y. Xu, X.Y. Shi, W. Huang, T.Y. Ruan, P. Xie, and J.L. Ding. 2013. M2-polarized tumor-associated macrophages promoted epithelial–mesenchymal transition in pancreatic cancer cells, partially through TLR4/IL-10 signaling pathway. *Lab. Invest.* 93:844–854. http://dx.doi.org/10.1038/labinvest.2013.69

Lowenfels, A.B., P. Maisonneuve, G. Cavallini, R.W. Ammann, P.G. Lankisch, J.R. Andersen, E.P. Dimagno, A. Andrén-Sandberg, and L. Domellöf. International Pancreatitis Study Group. 1993. Pancreatitis and the risk of pancreatic cancer. *N. Engl. J. Med.* 328:1433–1437. http://dx.doi.org/10.1056/NEJM199305203282001

Lowenfels, A.B., P. Maisonneuve, E.P. DiMagno, Y. Elitsur, L.K. Gates Jr., J. Perrault, and D.C. Whitcomb. International Hereditary Pancreatitis Study Group. 1997. Hereditary pancreatitis and the risk of pancreatic cancer. *J. Natl. Cancer Inst.* 89:442–446. http://dx.doi.org/10.1093/jnci/89.6.442

Lugrin, J., R. Parapanov, N. Rosenblatt-Velin, S. Rignault-Clerc, F. Feihl, B. Waeber, O. Müller, C. Vergely, M. Zeller, A. Tardivel, et al. 2015. Cutting edge: IL-1α is a crucial danger signal triggering acute myocardial inflammation during myocardial infarction. *J. Immunol.* 194:499–503. http://dx.doi.org/10.4049/jimmunol.1401948

McAllister, F., J.M. Bailey, J. Alsina, C.J. Nirschl, R. Sharma, H. Fan, Y. Rattigan, J.C. Roeser, R.H. Lankapalli, H. Zhang, et al. 2014. Oncogenic Kras activates a hematopoietic-to-epithelial IL-17 signaling axis in preinvasive pancreatic neoplasia. *Cancer Cell.* 25:621–637. http://dx.doi.org/10.1016/j.ccr.2014.03.014

Ochi, A., C.S. Graffeo, C.P. Zambirinis, A. Rehman, M. Hackman, N. Fallon, R.M. Barilla, J.R. Henning, M. Jamal, R. Rao, et al. 2012a. Toll-like receptor 7 regulates pancreatic carcinogenesis in mice and humans. *J. Clin. Invest.* 122:4118–4129. http://dx.doi.org/10.1172/JCI63606

Ochi, A., A.H. Nguyen, A.S. Bedrosian, H.M. Mushlin, S. Zarbakhsh, R. Barilla, C.P. Zambirinis, N.C. Fallon, A. Rehman, Y. Pylayeva-Gupta, et al. 2012b. MyD88 inhibition amplifies dendritic cell capacity to promote pancreatic carcinogenesis via Th2 cells. *J. Exp. Med.* 209:1671–1687. http://dx.doi.org/10.1084/jem.20111706

Pardoll, D.M. 2012. The blockade of immune checkpoints in cancer immunotherapy. *Nat. Rev. Cancer.* 12:252–264. http://dx.doi.org/10.1038/nrc3239

Pollard, J.W. 2004. Tumour-educated macrophages promote tumour progression and metastasis. *Nat. Rev. Cancer.* 4:71–78. http://dx.doi.org/10.1038/nrc1256

Pylayeva-Gupta, Y., K.E. Lee, C.H. Hajdu, G. Miller, and D. Bar-Sagi. 2012. Oncogenic Kras-induced GM-CSF production promotes the development of pancreatic neoplasia. *Cancer Cell.* 21:836–847. http://dx.doi.org/10.1016/j.ccr.2012.04.024

Rahib, L., J.M. Fleshman, L.M. Matrisian, and J.D. Berlin. 2016. Evaluation of pancreatic cancer clinical trials and benchmarks for clinically meaningful future trials: A systematic review. *JAMA Oncol.* 2:1209–1216. http://dx.doi.org/10.1001/jamaoncol.2016.0585

Salcedo, R., A. Worschech, M. Cardone, Y. Jones, Z. Gyulai, R.-M. Dai, E. Wang, W. Ma, D. Haines, C. O'hUigin, et al. 2010. MyD88-mediated signaling prevents development of adenocarcinomas of the colon: role of interleukin 18. *J. Exp. Med.* 207:1625–1636. http://dx.doi.org/10.1084/jem.20100199

Seifert, L., G. Werba, S. Tiwari, N.N. Giao Ly, S. Alothman, D. Alqunaibit, A. Avanzi, R. Barilla, D. Daley, S.H. Greco, et al. 2016a. The necrosome promotes pancreatic oncogenesis via CXCL1 and Mincle-induced immune suppression. *Nature.* 532:245–249. http://dx.doi.org/10.1038/nature17403

Seifert, L., G. Werba, S. Tiwari, N.N. Giao Ly, S. Nguy, S. Alothman, D. Alqunaibit, A. Avanzi, D. Daley, R. Barilla, et al. 2016b. Radiation therapy induces macrophages to suppress T-cell responses against pancreatic tumors in mice. *Gastroenterology.* 150:1659–1672.e5. http://dx.doi.org/10.1053/j.gastro.2016.02.070

Steele, C.W., S.A. Karim, J.D. Leach, P. Bailey, R. Upstill-Goddard, L. Rishi, M. Foth, S. Bryson, K. McDaid, Z. Wilson, et al. 2016. CXCR2 inhibition profoundly suppresses metastases and augments immunotherapy in pancreatic ductal adenocarcinoma. *Cancer Cell.* 29:832–845. http://dx.doi.org/10.1016/j.ccell.2016.04.014

Vandanmagsar, B., Y.H. Youm, A. Ravussin, J.E. Galgani, K. Stadler, R.L. Mynatt, E. Ravussin, J.M. Stephens, and V.D. Dixit. 2011. The NLRP3 inflammasome instigates obesity-induced inflammation and insulin resistance. *Nat. Med.* 17:179–188. http://dx.doi.org/10.1038/nm.2279

Yadav, D., and A.B. Lowenfels. 2013. The epidemiology of pancreatitis and pancreatic cancer. *Gastroenterology.* 144:1252–1261. http://dx.doi.org/10.1053/j.gastro.2013.01.068

Zaki, M.H., K.L. Boyd, P. Vogel, M.B. Kastan, M. Lamkanfi, and T.D. Kanneganti. 2010. The NLRP3 inflammasome protects against loss of epithelial integrity and mortality during experimental colitis. *Immunity.* 32:379–391. http://dx.doi.org/10.1016/j.immuni.2010.03.003

Zambirinis, C.P., E. Levie, S. Nguy, A. Avanzi, R. Barilla, Y. Xu, L. Seifert, D. Daley, S.H. Greco, M. Deutsch, et al. 2015. TLR9 ligation in pancreatic stellate cells promotes tumorigenesis. *J. Exp. Med.* 212:2077–2094. http://dx.doi.org/10.1084/jem.20142162

Zhang, L., G. Wu, F. Herrle, M. Niedergethmann, and M. Keese. 2012. Single nucleotide polymorphisms of genes for EGF, TGF-β and TNF-α in patients with pancreatic carcinoma. *Cancer Genomics Proteomics.* 9:287–295.

Zheng, L., J. Xue, E.M. Jaffee, and A. Habtezion. 2013. Role of immune cells and immune-based therapies in pancreatitis and pancreatic ductal adenocarcinoma. *Gastroenterology.* 144:1230–1240. http://dx.doi.org/10.1053/j.gastro.2012.12.042